Plasma membrane insertion of the AMPA receptor GluA2 subunit is regulated by NSF binding and Q/R editing of the ion pore

Yoichi Araki, Da-Ting Lin[1], and Richard L. Huganir[2]

Department of Neuroscience and Howard Hughes Medical Institute, Johns Hopkins University School of Medicine, Baltimore, MD 21205

Contributed by Richard L. Huganir, May 13, 2010 (sent for review April 16, 2010)

The delivery of AMPA receptors to the plasma membrane is a critical step both for the synaptic delivery of these receptors and for the regulation of synaptic transmission. To directly visualize fusion events of transport vesicles containing the AMPA receptor GluA2 subunit with the plasma membrane we used pHluorin-tagged GluA2 subunits and total internal reflection fluorescence microscopy. We demonstrate that the plasma membrane insertion of GluA2 requires the NSF binding site within its intracellular cytoplasmic domain and that RNA editing of the Q/R site in the ion channel region plays a key role in GluA2 plasma membrane insertion. Finally, we show that plasma membrane insertion of heteromeric GluA2/3 receptors follows the same rules as homomeric GluA2 receptors. These results demonstrate that the plasma membrane delivery of GluA2 containing AMPA receptors is regulated by its unique structural elements.

glutamate receptors | membrane trafficking | synapse | synaptic plasticity

Glutamate is the major excitatory neurotransmitter in the mammalian CNS. Ionotropic glutamate receptors are classified into several groups: AMPA, kainate, and NMDA receptors. AMPA receptors (AMPARs) are ligand-gated cation channels that mediate the majority of the fast excitatory synaptic transmission (1), whereas NMDA receptors (NMDARs) are critical for the induction of specific forms of synaptic plasticity by dynamically regulating synaptic expression of AMPARs (2–4).

The AMPARs consist of four subunits; GluA1, -2, -3, and -4 (5, 6). Several studies have shown that GluA2 interacts with PDZ domain containing proteins such as GRIP1/2 and PICK1 via its PDZ ligand at its C terminus. GRIP1/2 stabilizes surface expression of GluA2 or promotes receptor recycling to the plasma membrane (7, 8), whereas PICK1 promotes GluA2 endocytosis or inhibits receptor recycling to the plasma membrane (9–12). Disrupting GluA2-PICK1 interactions blocks the expression of both hippocampal and cerebellar LTD (11, 12). In contrast, N-ethylmaleimide-sensitive factor (NSF), an essential component of SNARE-mediated membrane fusion machinery (13–15), binds to the GluA2 juxtamembrane region (16–19). Disruption of NSF binding to GluA2 by a peptide inhibitor decreases both AMPAR mediated synaptic transmission (16, 17) and GluA2 surface expression by disassembling GluA2-PICK1 complexes (20), whereas overexpression of NSF increases surface expression of GluA2 (21). However, the precise regulatory mechanisms underlying GluA2 delivery to the surface plasma membrane remain elusive, mainly because exocytosis and endocytosis of AMPAR containing vesicles are highly dynamic and have not been kinetically resolved. Most conventional assays for monitoring AMPARs surface expression, including surface biotinylation or surface staining using antibodies against extracellular domains or extracellular tags, lack sufficient temporal resolution to isolate the kinetics of insertion. Therefore, direct visualization of plasma membrane insertion GluA2 containing receptors is a prerequisite to separate exocytotic events from rapid endocytosis of the receptors. Here, we visualize plasma membrane insertion of GluA2 containing vesicles by imaging superecliptic pHluorin-tagged GluA2 in neurons under total internal reflection fluorescence (TIRF) microscopy. Using this approach, we visualize individual insertion events of GluA2 containing vesicles. These events are blocked by tetanus toxin light chain indicating that they are mediated by SNARE machinery containing synaptobrevin (VAMP-2). We further demonstrated that approximately 50% of newly inserted GluA2 originate from recycling endosomes. We find that both the RNA editing of the Q/R site in the pore region of GluA2/3 and the NSF binding site of GluA2 strongly regulate surface delivery of AMPARs. These results describe the regulation of the insertion of GluA2 into the plasma membrane by distinct structural elements of the GluA2 subunit critical for the synaptic delivery of GluA2 containing AMPA receptors.

Results

Direct Visualization of GluA2 Insertion Events. To directly visualize GluA2 plasma membrane insertion in hippocampal neurons, we used total internal reflection microcopy (TIRFM) to image the fluorescence signal of superecliptic pHluorin-tagged GluA2 (pH-GluA2) near the cell surface. TIRFM allows excitation light to reach approximately 100 nm from the cover glass surface, enabling tracking of pHluorin-tagged receptor insertion at the plasma membrane. Moreover, the fluorescence of the pHluorin tag is quenched in the lumen of intracellular acidic organelles, including endosomal and Golgi compartments and is only detectable when these vesicles fuse with the plasma membrane and are exposed to the neutral pH of the extracellular environment (22). Thus, by imaging pH-GluA2 under TIRFM, one can visualize newly inserted cell surface pHluorin-tagged AMPA receptors (23, 24). Using TIRF imaging pH-GluA2 signals were detected distributed on the cell body and dendrites at steady state. After complete bleaching of the preexisting pH-GluA2 signal on the cell surface to increase the signal to noise ratio, we were able to visualize many individual insertion events over a 10-min recording period (Fig. 1*A1*). An example of an image sequence of GluA2 insertion is shown in Fig. 1*A2*. In the image sequence shown the cells were imaged every 5 sec (Movie S1). As shown in Fig. 1*A2* GluA2 fluorescence appeared and laterally diffused from the point of insertion within the plasma membrane. The average signal intensity at the center of the insertion spot (blue: diameter 1 μm), the medium proximal region surrounding the insertion point (pink: 4 μm), and the distal region (green: 8 μm) is shown in Fig. 1*A3* demonstrating that the newly inserted GluA2 rapidly diffused radially from the point of insertion. Y–t rendering images were generated by rotating the original x-y-t stack 90° along the

Author contributions: Y.A., D.-T.L., and R.L.H. designed research; Y.A. and D.-T.L. performed research; Y.A., D.-T.L., and R.L.H. contributed new reagents/analytic tools; Y.A. and R.L.H. analyzed data; and Y.A., D.-T.L., and R.L.H. wrote the paper.

The authors declare no conflict of interest.

[1]Present address: The Jackson Laboratory, Bar Harbor, ME 04609.

[2]To whom correspondence should be addressed. E-mail: rhuganir@jhmi.edu.

This article contains supporting information online at www.pnas.org/lookup/suppl/doi:10.1073/pnas.1006584107/-/DCSupplemental.

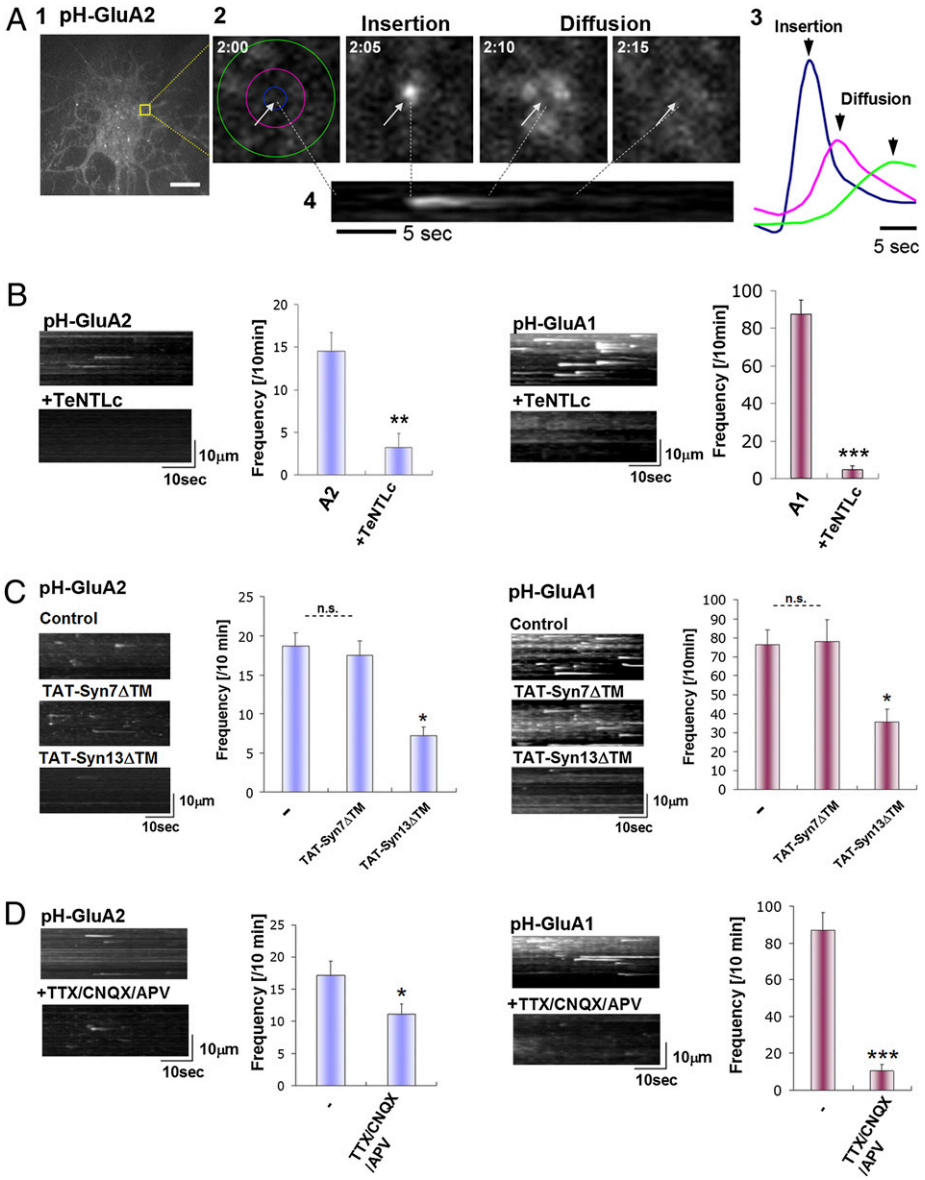

Fig. 1. Direct imaging of GluA2 plasma membrane insertion events. (*A*) Representative images of GluA2 insertion events (1). Detection of pH-GluA2 insertion events over a 10-min time period in hippocampal neurons visualized using TIRF microscopy (Scale bar, 10 μm.) (2). Representative images of the time course of pH-GluA2 insertion and diffusion (3). Quantification of fluorescence change over time demonstrates lateral diffusion of pH-GluA2 following insertion (4). Y–t projection image shows MIP of the insertion event shown in (2) and (3). (*B*) Insertion of GluA1 and GluA2 is dependent of VAMP2. Cotransfection of TeNTLc abolished both GluA1 and GluA2 insertion events. Examples of the MIPs and quantitation of the insertion events are shown (means ± SEM, $n = 12$). (*C*) Effect of recycling inhibitor (TAT-Syn7/13ΔTM) on GluA1 and 2 insertion events frequency per 10 min. Only TAT-Syn13 ΔTM reduced both GluA1 and 2 insertion. Examples of the MIPs and quantitation of the insertion events are shown (means ± SEM, $n = 10$). (*D*) Acute activity block (TTX/CNQX/APV treatment) abolished most of GluA1 insertion, whereas this treatment had a smaller effect on GluA2 insertion. Examples of the MIPs and quantitation of the insertion events are shown (means ± SEM, $n = 11$).

y axis, and the maximum intensity of each x line was projected onto a single pixel of the *y* axis using a maximum intensity projection (MIP) algorithm (Fig. 1*A4*) to show the frequency and time course of the insertion events.

We verified these as true GluA2 receptors insertion events by coexpressing tetanus toxin light chain (TeNTLc) (25) (Fig. 1*B*). TeNTLc cleaves synaptobrevin/VAMP2, an essential component of the SNARE complex, and thus inhibits synaptobrevin/VAMP2 mediated exocytosis. TeNTLc abolished both GluA2 insertion events (pH-GluA2+vector: 14.5 ± 3.2 events/10 min, pH-GluA2+TeNTLc: 3.6 ± 0.9 events/10 min), as well as GluA1 insertion events (pH-GluA1+vector: 87.5 ± 7.7 events/10 min, pH-GluA1+TeNTLc 4.8 ± 1.9 events/10 min), confirming that these events represent newly inserted AMPA receptors delivered via SNARE mediated exocytosis (26). The fluorescence intensity of the GluA1 and GluA2 insertion events were quite different [12,265 ± 1,595 for GluA1: 1,769 ± 549 for GluA2 (means ± SD): Movie S1] suggesting that the GluA2 insertion events contain fewer receptors than the GluA1 events.

AMPARs required for LTP expression are thought to originate from recycling endosomes (27). Perfusion of TAT-Syn13ΔTM peptide, which blocks transport of recycling endosomes to the plasma membrane, inhibited approximately 50% of both GluA1 and 2 insertion, whereas perfusion of TAT-Syn7ΔTM, a blocker of transport from early endosomes to late endosomes did not affect either GluA1 or 2 exocytosis (Fig. 1*C*). These results in-

dicate that a substantial fraction of the newly inserted AMPARs (both GluA1 and 2) originate from recycling endosomes.

We investigated whether neuronal activity can affect GluA1 and 2 receptor insertion frequency (Fig. 1*D*). Acute blocking of neuronal activity by application of TTX/CNQX/APV for 15 min abolished approximately 88% of GluA1 insertion (basal: 87.2 ± 9.6 events/10 min, TTX/CNQX/APV: 10.5 ± 3.4 events/10 min), whereas this treatment reduced GluA2 insertion only by approximately 30% (basal: 17.2 ± 2.2 events/10 min, TTX/CNQX/APV: 11.2 ± 1.6 events/10 min). These results suggest that, under these conditions, GluA1 insertion is activity-dependent and GluA2 is mostly constitutive.

NSF Binding Site of GluA2 Is Critical for GluA2 Insertion Events. Previous studies have shown that the intracellular C-terminal domains of AMPAR subunits bind many proteins that regulate AMPAR membrane trafficking (28). We therefore examined if the GluA2 C-terminal domain was important for the insertion events. Initially, we used serial C-terminal deletions to identify regions required for GluA2 exocytosis (Fig. 2*A*). We found that C-terminal truncation to amino acid 856 (856t) did not affect the rate of GluA2 exocytosis, whereas C-terminal truncation to residue 847 (847t) abolished GluA2 exocytosis (Fig. 2*B*). This region (848–856) contains the binding site for the NSF protein, a site present only in the GluA2 C termini and not other AMPAR subunits. To confirm that NSF binding to GluA2 is important for basal GluA2 insertion, we next used point mutations (V848L/A849T/P852T) that specifically eliminate NSF binding to GluA2 (29). As shown in Fig. 2*C,* these point mutations abolish the GluA2 insertion events observed by TIRFM.

RNA Editing of the Q/R Site Within the Ion Channel Pore Regulates GluA2 Insertion Events. Another structural element unique to the GluA2 subunit is the Q/R RNA editing site within the ion channel pore region. Most GluA2 subunits are RNA edited to encode an R instead of a Q in this site. Previous studies have reported that the edited form of GluA2 is retained in the ER and exhibits decreased cell surface expression compared with the unedited form, which exits from the ER and traffics efficiently to the cell surface (30). Thus, we wanted to examine the role of editing on the rate of GluA2 surface insertion. Interestingly, the unedited GluA2 (R607Q) had an enhanced rate of GluA2 insertion compared with the edited version (Fig. 2*C*). We also examined the unedited version of GluA2 (R607Q) in combination with NSF binding mutant to examine how these sites may interact. We found that the NSF binding site is also critical for plasma membrane insertion of the unedited GluA2 (Fig. 2*C*).

Effect of NSF Binding Site and Q/R Editing on GluR2 Steady-State Surface Expression. To investigate whether these structural elements are also required for GluA2 surface expression in neurons, we infected hippocampal neurons with Sindbis viruses expressing different GluA2 mutants and conducted surface biotinylation assays (Fig. 3*A*). After 24 h of infection, surface biotinylated proteins were precipitated by Streptoavidin-beads. Mutation of the NSF binding reduced surface expression of GluA2, whereas the R607Q mutation facilitated surface expression. GluA2 containing both mutations (R607Q/ΔNSF) also showed reduced surface expression of GluA2 compared with R607Q, again indicating that the NSF binding site affects surface expression levels of edited and unedited GluA2.

As a complementary method to determine requirements for GluA2 surface delivery in neurons, we modified pH-GluA2 to insert a thrombin cleavage sequence (LVPRGS) between the pHluorin-tag and GluA2 sequence (designated as pH-T-GluA2). Surface delivery of pH-T-GluA2 can be monitored using a thrombin cleavage assay (31, 32) to study the kinetics of AMPA receptor surface delivery (Fig. 3*B*). Thrombin pretreatment cleaves preexisting surface pH-T-GluA2 receptors to allow specific detection of subsequently inserted receptors. After thoroughly washing the coverslip, cells were placed into conditioned media for the indicated times. Newly inserted GluA2 subunits were visualized by surface staining using anti-GFP antibody and Alexa546 conjugated secondary anti-rabbit IgG antibody. The

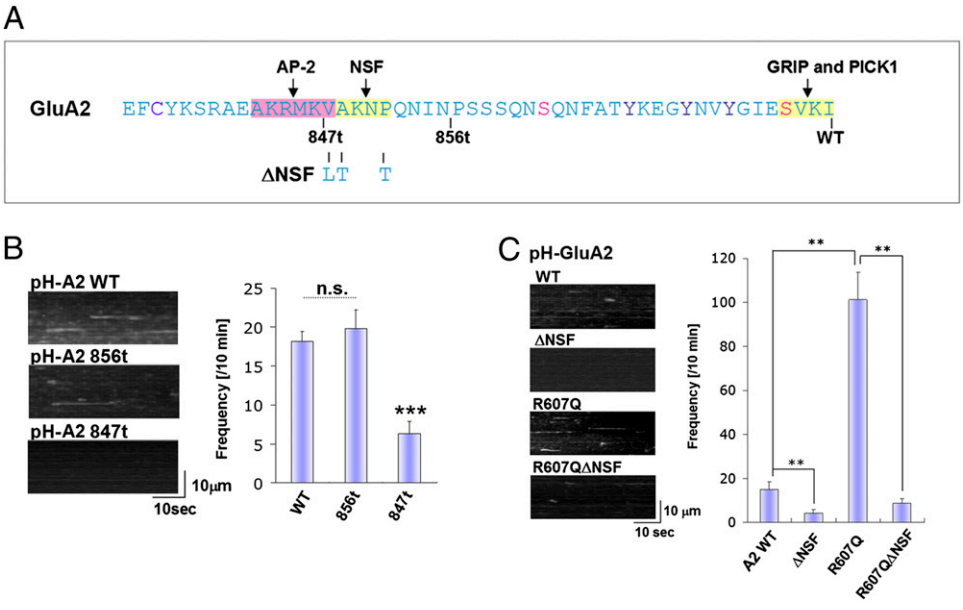

Fig. 2. The NSF binding site is important for GluA2 insertion. (*A*) Mapping of GluA2 C-terminal region responsible for efficient insertion. GluA2 C-terminal sequence; the truncation and point mutants used in this study are indicated. (*B*) The GluA2 856t mutant has no effect on GluA2 insertion, whereas GluA2 847t mutant abolished its insertion. Examples of the MIPs and quantitation of the insertion events are shown (means ± SEM, $n = 12$). (*C*) Effect of GluA2 ΔNSF and R607Q to GluA2 insertion frequency. Mutation of the NSF site and the Q/R site significantly affect the insertion frequency. Examples of the MIPs and quantitation of the insertion events are shown (means ± SEM, $n = 14$).

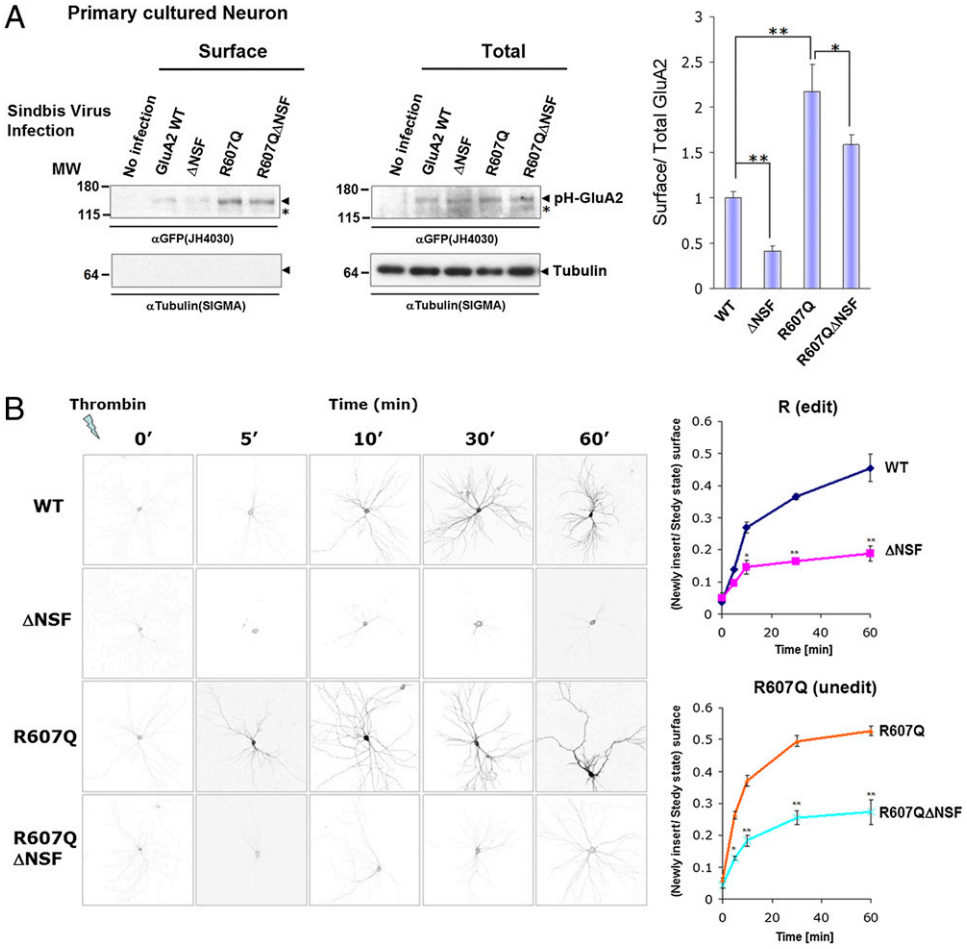

Fig. 3. The NSF binding site is important for efficient delivery of GluA2 to plasma membrane. (*A*) Surface expression of GluA2 constructs in hippocampal neurons probed using a surface biotinylation assay. Hippocampal neurons were infected with Sindbis virus expressing the indicated GluA2 construct and the surface receptor analyzed using biotinylation techniques. The surface fraction precipitated by streptoavidin-beads (surface) and the total lysate (total) is shown. The graph shows the ratio of surface GluA2/total GluA2 (means ± SEM, $n = 3$). (*B*) Newly inserted GluA2 time course. Neurons expressing pH-GluA2 were treated by Thrombin for 5 min. After thoroughly washing the coverslip, the cells were incubated for the indicated times. The graph shows the recovery of surface receptors over time (means ± SEM, $n = 3$, each time point). We set steady state ratio of surface/total GluA2 is 1.

ΔNSF GluA2 mutant showed reduced kinetics of surface delivery of GluA2 both in edited and unedited (R607Q) forms. These results indicate that the NSF binding sequence is indispensable for efficient trafficking of GluA2 to the cell surface.

Presence of the NSF Binding Site and an Unedited Q/R Site Is Required for Efficient Insertion of GluA2/3 Heteromers. To visualize GluA3 insertion, pHluorin-tagged GluA3 subunits were transfected into hippocampal neurons and imaged by TIRF microscopy. As shown in Fig. 4*A*, compared with GluA1, both GluA2 and 3 have lower insertion frequencies (GluA1 87.5 ± 7.7 events/10 min: GluA2 14.6 ± 3.2 events/10 min: GluA3 14.1 ± 5.8 events/10 min). We used the edited version (R) of GluA2 (pH-GluA2$_{/R}$) for comparison because the majority of GluA2 in the mature brain is edited (R) (designated as GluA2$_{/R}$), whereas GluA1 and 3 are unedited (Q) (designated as GluA1$_{/Q}$, GluA3$_{/Q}$, respectively). To further investigate the mechanisms of GluA2/3 exocytosis, we coexpressed pH-GluA2$_{/R}$ with various GluA3 constructs, and examined pH-GluA2$_{/R}$ exocytosis (Fig. 4*B*). Interestingly, coexpression of GluA3$_{/Q}$ greatly facilitates GluA2$_{/R}$ insertion (pH-GluA2$_{/R}$+Vector: 13.0 ± 2.7events/10 min, pH-GluA2$_{/R}$+GluA3$_{/Q}$ 130.1 ± 14.1events/10 min: $^{**}P < 0.01$), whereas coexpression of pH-GluA2$_{/R}$ with a construct containing a artificial edited mutation in GluA3 pore region (Q612R) had no effect (pH-GluA2$_{/R}$+ R3 Q612R 16.0 ± 6.6 events/10 min: $P = 0.58$ compared with pH-GluA2$_{/R}$ + mock vector). This result suggests that the presence of unedited residue (Q) in an AMPAR complex is critical for receptor surface delivery. Deletion of the complete C-terminal region of GluA3 (GluA3$_{/Q}$ΔC) did not inhibit the enhancing effect of GluA3$_{/Q}$ on pH-GluA2$_{/R}$ insertions [pH-GluA2$_{/R}$+ GluA3$_{/Q}$ΔC 116.0 ± 19.8 events/10 min ($P = 0.10$) compared with pH-GluA2$_{/R}$ + GluA3$_{/Q}$], indicating that GluA3 C-terminal sequence is not critical for the ability of GluA3$_{/Q}$ to facilitate GluA2 exocytosis. These results indicate that facilitation of edited GluA2 insertion by GluA3 depends on the unedited residue (Q) of GluA3.

We examined the importance of NSF binding sequence for heteromeric receptor (GluA2/3) surface delivery (Fig. 4*C*). Coexpressing GluA3$_{/Q}$ with pH-GluA2$_{/R}$ ΔNSF had no effect in GluA2 exocytosis (pH-GluA2$_{/R}$ ΔNSF+Vector 4.3 ± 1.7 events/10 min: pH-GluA2$_{/R}$ΔNSF+GluA3$_{/Q}$ 7.5 ± 1.9 events/10 min: $P = 0.26$). To test whether the NSF binding site had to be present in the GluA2 subunit we generated GluA3$_{/Q}$ mutants that can artificially interact with NSF (GluA3$_{/Q}$ NSF^{+}) by mutating GluA3 to contain a NSF binding site identical to GluA2 (L853V/T854A/T857P) (29). Coexpressing GluA3$_{/Q}$NSF^{+} with pH-GluA2$_{/R}$ ΔNSF could rescue the GluA2$_{/R}$ ΔNSF insertion deficiency (pH-GluA2$_{/R}$ΔNSF+GluA3$_{/Q}$NSF^{+} 101.5 ± 9.5 events/10 min:

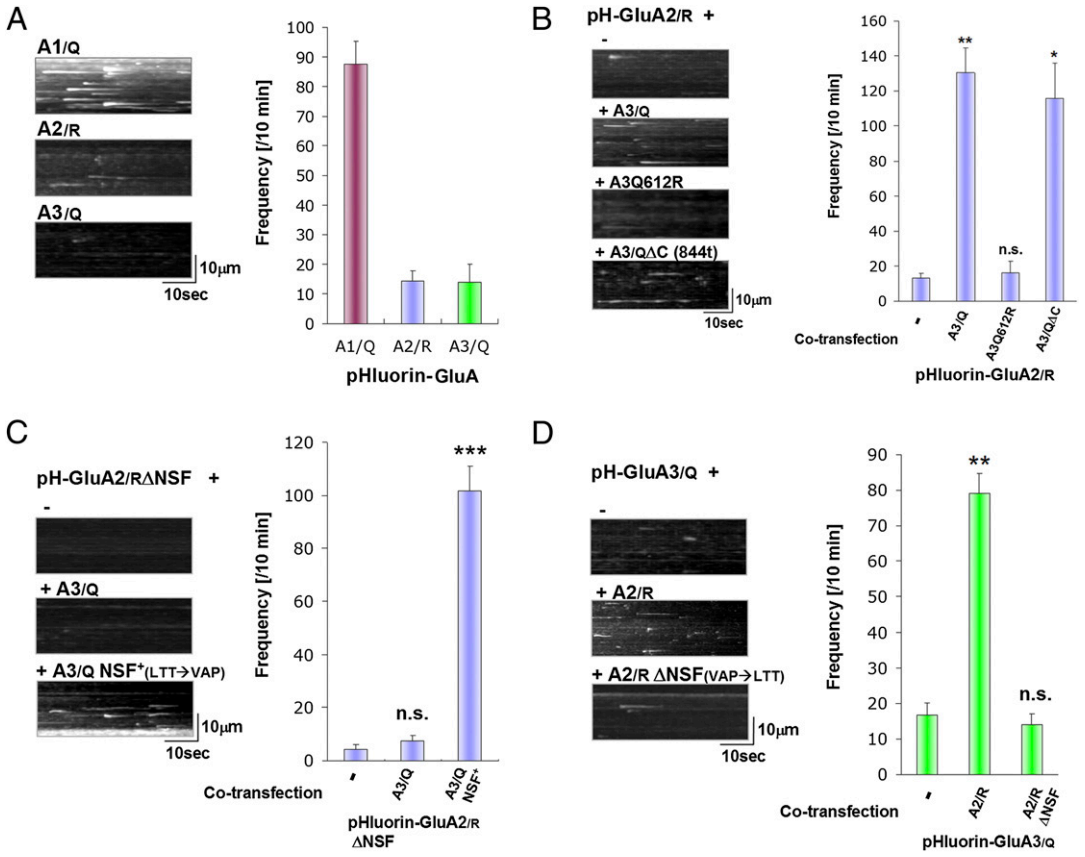

Fig. 4. The NSF binding site and unedited residue (Q) is required for efficient insertion of GluA2/3 heteromers. (*A*) Insertion frequency for pH-GluA1$_{/Q}$, GluA2$_{/R}$, GluA3$_{/Q}$ when they were expressed alone in hippocampal neurons. R or Q indicates edited (R) or unedited (Q) amino acid in pore region of each AMPA receptor subunits. Examples of the MIPs and quantitation of the insertion events are shown (means ± SEM, n = 11). (B) Effect of GluA3 coexpression for GluA2$_{/R}$ insertion frequency. Examples of the MIPs and quantitation of the insertion events are shown (means ± SEM: n = 11). (*C*) Effect of coexpression of GluA3$_{/Q}$ containing an artificial NSF binding sequence on GluA2$_{/R}$ ΔNSF insertion frequency. Examples of the MIPs and quantitation of the insertion events are shown (means ± SEM, n = 12). (*D*) Effect of GluR2 coexpression for pH-GluA3$_{/Q}$ insertion events. GluA2 carrying the NSF binding sequence facilitates GluA3 insertion event frequency. Examples of the MIPs and quantitation of the insertion events are shown (means ± SEM, n = 12).

$P < 0.001$ compared with pH-GluA2$_{/R}$ΔNSF + vector), indicating that both the NSF binding sequence and an unedited residue (Q) is required for efficient insertion of GluA2/3 heteromeric receptors. Interestingly, these sites can be in either the GluA2 or the GluA3 subunits in any combination, in cis or trans, and still have their effect on insertion frequency.

Finally, we also investigated the effect of GluA2 coexpression in GluA3 surface delivery (Fig. 4*D*). Coexpression of GluA2$_{/R}$ with pH-GluA3$_{/Q}$ dramatically increased the insertion frequency of GluA3 (pH-GluA3$_{/Q}$+Vector 16.8 ± 3.4 events/10 min, pH-GluA3$_{/Q}$+GluA2$_{/R}$ 79.3 ± 5.5 events/10 min: $P < 0.01$). However, coexpression of GluA2$_{/R}$ ΔNSF did not have this facilitating effect (pH-GluA3$_{/Q}$+GluA2ΔNSF 14.0 ± 3.2 events/10 min: $P = 0.58$ compared with pH-GluA3$_{/Q}$+Vector). Therefore, the NSF binding sequence from GluA2$_{/R}$ is essential for efficient surface delivery of GluA3$_{/Q}$.

Discussion

We have directly visualized the plasma membrane insertion of GluA2/3 containing intracellular vesicles by imaging superecliptic pHluorin-tagged AMPARs using TIRFM. We have shown (*i*) GluA2 plasma membrane insertion events contain only a few receptors compared with that of GluA1; (*ii*) GluA2 insertion events can be blocked by tetanus toxin light chain, indicating that they are mediated by synaptobrevin/VAMP-2 containing SNARE machinery; (*iii*) approximately 50% of GluA1 and 2 insertion events originate from recycling endosomes; (*iv*) GluA1 exocytosis is mostly (approximately 88%) activity dependent, whereas GluA2 exocytosis is largely (approximately 70%) constitutive, but approximately 30% of GluA2 exocytosis remains activity-dependent; (*v*) Both the NSF binding sequence in the GluA2 C terminus and a unedited residue (Q) in the pore region facilitate GluA2 receptor surface insertion; (*vi*) and GluA2/3 heteromeric receptors behave similarly to GluA2 homomers and the insertion of GluA2/3 heteromers requires the NSF binding site in GluA2 and the unedited Q/R site in GluA3.

Previous studies have shown that the editing of the Q/R residue in the pore region of GluA2 plays an important role in the assembly of GluA2 subunits and the exit of GluA2 subunits from the ER (30). Overexpression of the GluA2$_{/R}$ subunits results in ER retention of the GluA2 subunit, whereas overexpressed GluA2$_{/Q}$ subunits are not retained in the ER. Interestingly, our data demonstrates that editing of this site dramatically decreases the rate of the direct insertion of GluA2 into the plasma membrane analyzed by TIRFM and pH-GluA2. This may be due to an increase in the pool of GluA2$_{/Q}$ in intracellular vesicles able to fuse with the plasma membrane because of the lack of retention of the GluA2$_{/Q}$ subunit in the ER. Alternatively, editing the Q/R site may have a direct independent effect on the insertion of the GluA2 subunit into the plasma membrane.

Disrupting the interaction between GluA2 and NSF results in the rundown of AMPA responses in neurons, suggesting that NSF is important for incorporation and maintenance of AMPARs at synapses (16, 17, 29). Recent studies have suggested that NSF may

regulate the delivery and/or lateral mobility of GluA2 containing receptors from extrasynaptic sites to synapses (32). Our results clearly show that the direct plasma membrane insertion of GluA2 is also regulated by NSF binding.

A schematic model of GluA2/3 receptor surface expression requirements is shown in Fig. S1. In the brain, most GluA2 is edited at the Q/R site in the ion channel pore (33, 34), Thus, heteromerization of $GluA2_{/R}$ with $GluA3_{/Q}$ can provide unedited residues into the AMPAR complex to stimulate GluA2/3 receptors surface insertion. Reciprocally, GluA3 does not bind NSF and thus it is not efficiently trafficked to the cell surface. Indeed, although overexpressed GFP-GluA3 can be observed in spines, synaptic transmission mediated by this overexpressed GluA3 cannot be detected, possibly because it is not inserted into the synaptic membrane surface (35). Similarly, overexpressed GluA3 in cerebellar Purkinje cells is not incorporated into synapses unless mutated to contain an NSF binding site (29). Interestingly, unedited GluA3 homomeric receptors are calcium permeable, which could lead to excitotoxicity and may cause neuronal cell death. The low efficiency of surface delivery of calcium permeable (unedited) GluA3 may provide an intrinsic neuroprotective mechanism to prevent the insertion of high levels of calcium permeable AMPAs.

The results presented here reveal insights into the regulation of GluA2 plasma membrane insertion under basal conditions. It will be interesting to use similar methods to investigate whether the same or additional molecular mechanisms control AMPAR insertion during forms of synaptic plasticity such as LTP.

Materials and Methods

Detailed experimental methods are described in *SI Materials and Methods*. The use and care of animal in this study follows the guideline of the Institutional Animal Care and Use Committee at the Johns Hopkins University.

Chemicals, Molecular Biology. All restriction enzymes were from New England Biolabs. Chemicals were obtained from SIGMA-Aldrich unless otherwise specified. TTX, NBQX, and APV were from TOCRIS Bioscience. DNA sequencing was performed at the Johns Hopkins University School of Medicine Sequencing Facility.

Neuronal Cell Culture, Image Analysis, and Statistics. Hippocampal neuron cultures were prepared, maintained, and analyzed as previously described (23). Values were expressed as means ± SEM unless otherwise specified. Comparisons for two groups of data were done by two-tailed student's *t* test. Multiple comparisons were done by one-way ANOVA followed by Tukey posthoc test. (* $P < 0.05$, ** $P < 0.01$, *** $P < 0.001$). See *SI Materials and Method* for details.

Visualization of Receptor Insertion by Total Internal Reflection Microscopy. The TIRF microscopy imaging system was based on a Zeiss AxioObserver microscope (Carl Zeiss Microimaging) as previously described (23). Hippocampal neurons were transfected plasmid, and were imaged by TIRF microscopy. See *SI Materials and Methods* for details.

ACKNOWLEDGMENTS. We thank all Huganir Laboratory members for excellent technical assistance and critical discussions throughout this study and specifically Gareth Thomas for help with the writing of the manuscript. We also thank Mike Ehlers (Duke University) for kindly providing materials. This work is supported by National Institute of Health Grant R01NS036715. Y.A. was a recipient of research fellowship from the Japan Society of the Promotion of Science. R.L.H. is an investigator of the Howard Hughes Medical Institute.

1. Dingledine R, Borges K, Bowie D, Traynelis SF (1999) The glutamate receptor ion channels. *Pharmacol Rev* 51:7–61.
2. Malenka RC, Bear MF (2004) LTP and LTD: An embarrassment of riches. *Neuron* 44: 5–21.
3. Collingridge GL, Isaac JT, Wang YT (2004) Receptor trafficking and synaptic plasticity. *Nat Rev Neurosci* 5:952–962.
4. Bredt DS, Nicoll RA (2003) AMPA receptor trafficking at excitatory synapses. *Neuron* 40:361–379.
5. Hollmann M, Heinemann S (1994) Cloned glutamate receptors. *Annu Rev Neurosci* 17: 31–108.
6. Shepherd JD, Huganir RL (2007) The cell biology of synaptic plasticity: AMPA receptor trafficking. *Annu Rev Cell Dev Biol* 23:613–643.
7. Dong H, et al. (1997) GRIP: A synaptic PDZ domain-containing protein that interacts with AMPA receptors. *Nature* 386:279–284.
8. Osten P, et al. (2000) Mutagenesis reveals a role for ABP/GRIP binding to GluR2 in synaptic surface accumulation of the AMPA receptor. *Neuron* 27:313–325.
9. Xia J, Zhang X, Staudinger J, Huganir RL (1999) Clustering of AMPA receptors by the synaptic PDZ domain-containing protein PICK1. *Neuron* 22:179–187.
10. Chung HJ, Xia J, Scannevin RH, Zhang X, Huganir RL (2000) Phosphorylation of the AMPA receptor subunit GluR2 differentially regulates its interaction with PDZ domain-containing proteins. *J Neurosci* 20:7258–7267.
11. Seidenman KJ, Steinberg JP, Huganir R, Malinow R (2003) Glutamate receptor subunit 2 Serine 880 phosphorylation modulates synaptic transmission and mediates plasticity in CA1 pyramidal cells. *J Neurosci* 23:9220–9228.
12. Steinberg JP, et al. (2006) Targeted in vivo mutations of the AMPA receptor subunit GluR2 and its interacting protein PICK1 eliminate cerebellar long-term depression. *Neuron* 49:845–860.
13. Rothman JE (1994) Mechanisms of intracellular protein transport. *Nature* 372:55–63.
14. Haas A (1998) NSF—fusion and beyond. *Trends Cell Biol* 8:471–473.
15. Zhao C, Slevin JT, Whiteheart SW (2007) Cellular functions of NSF: Not just SNAPs and SNAREs. *FEBS Lett* 581:2140–2149.
16. Song I, et al. (1998) Interaction of the N-ethylmaleimide-sensitive factor with AMPA receptors. *Neuron* 21:393–400.
17. Nishimune A, et al. (1998) NSF binding to GluR2 regulates synaptic transmission. *Neuron* 21:87–97.
18. Noel J, et al. (1999) Surface expression of AMPA receptors in hippocampal neurons is regulated by an NSF-dependent mechanism. *Neuron* 23:365–376.
19. Osten P, et al. (1998) The AMPA receptor GluR2 C terminus can mediate a reversible, ATP-dependent interaction with NSF and alpha- and beta-SNAPs. *Neuron* 21:99–110.
20. Hanley JG, Khatri L, Hanson PI, Ziff EB (2002) NSF ATPase and alpha-/beta-SNAPs disassemble the AMPA receptor-PICK1 complex. *Neuron* 34:53–67.
21. Huang Y, et al. (2005) S-nitrosylation of N-ethylmaleimide sensitive factor mediates surface expression of AMPA receptors. *Neuron* 46:533–540.
22. Miesenböck G, De Angelis DA, Rothman JE (1998) Visualizing secretion and synaptic transmission with pH-sensitive green fluorescent proteins. *Nature* 394:192–195.
23. Lin DT, et al. (2009) Regulation of AMPA receptor extrasynaptic insertion by 4.1N, phosphorylation and palmitoylation. *Nat Neurosci* 12:879–887.
24. Yudowski GA, et al. (2007) Real-time imaging of discrete exocytic events mediating surface delivery of AMPA receptors. *J Neurosci* 27:11112–11121.
25. Eisel U, et al. (1993) Tetanus toxin light chain expression in Sertoli cells of transgenic mice causes alterations of the actin cytoskeleton and disrupts spermatogenesis. *EMBO J* 12:3365–3372.
26. Lu W, et al. (2001) Activation of synaptic NMDA receptors induces membrane insertion of new AMPA receptors and LTP in cultured hippocampal neurons. *Neuron* 29:243–254.
27. Park M, Penick EC, Edwards JG, Kauer JA, Ehlers MD (2004) Recycling endosomes supply AMPA receptors for LTP. *Science* 305:1972–1975.
28. Song I, Huganir RL (2002) Regulation of AMPA receptors during synaptic plasticity. *Trends Neurosci* 25:578–588.
29. Steinberg JP, Huganir RL, Linden DJ (2004) N-ethylmaleimide-sensitive factor is required for the synaptic incorporation and removal of AMPA receptors during cerebellar long-term depression. *Proc Natl Acad Sci USA* 101:18212–18216.
30. Greger IH, Khatri L, Ziff EB (2002) RNA editing at arg607 controls AMPA receptor exit from the endoplasmic reticulum. *Neuron* 34:759–772.
31. Passafaro M, Piëch V, Sheng M (2001) Subunit-specific temporal and spatial patterns of AMPA receptor exocytosis in hippocampal neurons. *Nat Neurosci* 4:917–926.
32. Beretta F, et al. (2005) NSF interaction is important for direct insertion of GluR2 at synaptic sites. *Mol Cell Neurosci* 28:650–660.
33. Seeburg PH, Higuchi M, Sprengel R (1998) RNA editing of brain glutamate receptor channels: Mechanism and physiology. *Brain Res Brain Res Rev* 26:217–229.
34. Sommer B, Köhler M, Sprengel R, Seeburg PH (1991) RNA editing in brain controls a determinant of ion flow in glutamate-gated channels. *Cell* 67:11–19.
35. Shi S, Hayashi Y, Esteban JA, Malinow R (2001) Subunit-specific rules governing AMPA receptor trafficking to synapses in hippocampal pyramidal neurons. *Cell* 105:331–343.